Evaluation of Fracture Toughness for Wood-Epoxy Adhesive System under External Shear Force*

Kohei KOMATSU**, Hikaru SASAKI** and Takamaro MAKU**

Abstract——Fracture Toughness G_c of Wood-Epoxy adhesive system under external shear force was evaluated by employing the experimental compliance method based on the Griffith-Irwin fracture theory.

Invariability of G_c with the different glue line length was tolerably recognized and the representative value of G_c for the above system was about 0.25 (cm·kg/cm^2) throughout the series of glue line thickness tested.

Fracture mode and stress distribution were discussed with some helps of Finite Element Method.

Introduction

Raptures of composite structures or members such as stressed skin panel or glulam are often initiated from the parts of adhesive joints. Therefore, members having adhesive-bonded parts should be designed depending on the reasonable fracture criterion of adhesive joint.

So called fracture strength obtained from the ordinary adhesive joint tests, in which the load carring capacity of adhesive joints is evaluated directly by the avarage fracture load or in many cases with the avarage fracture stress on the joint area, does not always give the reasonable standards for the fracture of adhesive joint, because these strength properties often vary with testing factors such as joint area, shape and dimensions of specimens, test speed etc.

When a certain combination of adhesive system is once selected, the material constant which dominates the fracture of the adhesive system is desired to be as consistent as possible throughout any variation of test fractors so that the adhesive system is used safely enough to structural members in which various joint configurations may be claimed.

The well known GRIFFITH[1]-IRWIN[2] fracture theory may give some hints to discuss such problems as fractures of adhesive bond, because of the analogus features between two cases of adhesive bond and homogeneous material with respect to both stress concentration at vicinity of geometrical irregularities and energy spent irreversibly through

* Presented partly at the 24th Annual Meeting of the Japan Wood Research Society, Tokyo, April, 1974.

** Division of Composite Wood.

separation of the interface as already interpreted by WILLIAMS[3].

In the field of adhesive bond, the off-set of adherends has been simulated as the geometrical irregularrity in many cases and the fracture energy approach has mainly employed to evaluate the material constant dominating the fracture of adhesive bond.

Many investigations have already verifyed that the Fracture Toughness (sometimes called as Toughness) G_c is material constant which is invariable through different joint geometries and test configurations[4~10]. Unfortunately, these verifications have almost been limited in case of cleavage force and adherend of non-woody materials.

In practice, adhesive bonds are often used in parts of wood construction subjected by shear force. Recently, WALSH[11] has discussed strength of the typical lap joint of wood by employing the approach of stress intensity factor neglecting the thickness of glue line. No more results have been obtained with respect to wood adhesive bonds subjected by external shear force.

This study was intended to verify the invariability of G_c for wood-epoxy adhesive system under external shear force, and was discussed with the GRIFFITH-IRWIN fracture theory.

Experimental

Preparation of Specimen

Process of preparation of the test specimen is shown in Fig. 1 and 2. In Fig. 1,

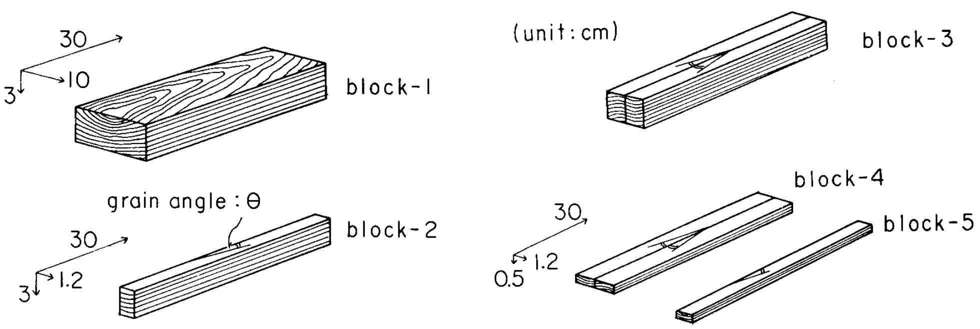

Fig. 1. Wood blocks and the machining process.

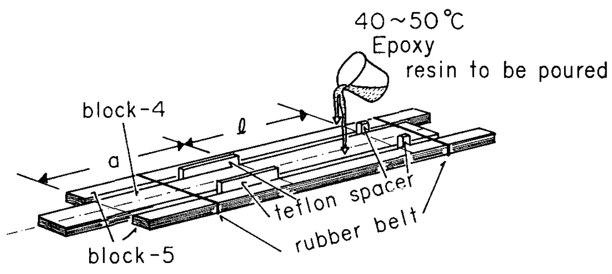

Fig. 2. Gluing process.

block-1 was cut from a flitch of air dried Lawson cypress (*Chamaecyparis Lawsoniana* PARL.) so that the grain direction always inclined about 2~4° in L–T plane to the edge of the block. The block-1 was cut into two block-2s with a mitre saw. Half numbers of the block-2 were paired and glued together with epoxy resin adhesives so as to make book-matched grain. The bonded blocks were called block-3. Then the block-3 and the rest of block-2 (unbonded) were sawn into 5~6 mm thick with a mitre saw. These strips were called block-4 and block-5 respectively. Then the block-4 and two block-5s were bound together so as to make conversing grains from left to right in Fig. 2 along the glue lines of which thickness and length were controlled with teflon spacers. The bottom of the glue line was sealed with cellulose tape before the resin was poured. Then the moderatelly warmed, bubble-free epoxy resin mixed with 11 phr (parts per hundred of resin by weight) of hardener DETA (Diethylene triamine) was poured carefully into the narrow cavities. After more than 24 hr. cured at 20°C and 60% R.H., specimens were finished with a super-surfacer into 4 mm thick. Splints of birch were bonded on the strip with same epoxy resin and the bonded strips were cut into the final form of specimen. Then, the specimens were conditioned at 20°C and 60%

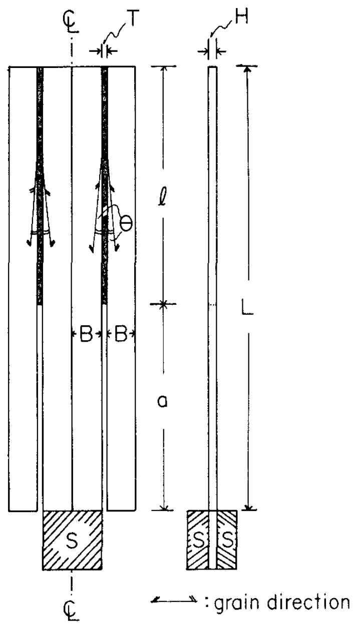

Fig. 3. Schematic diagrams of test specimen. *a*: *crack* length, *l*: glue line length, B: width of single adherend (1.2 cm), T: thickness of glue line, H: thickness of specimen (0.4 cm), S: splint (2.4×2.7×0.9 cm), *θ*: grain angle (2~4°), L: total length of specimen (25 cm)

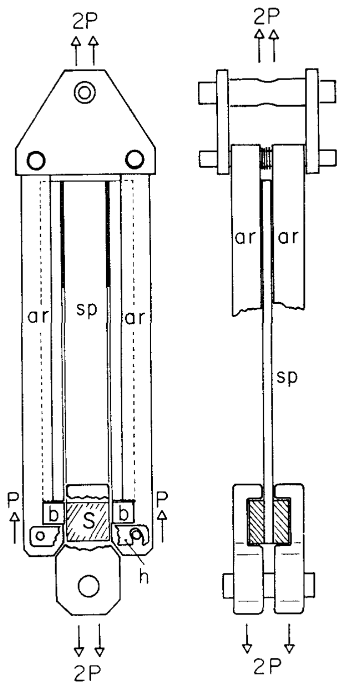

Fig. 4. Schematic diagrams of the test apparatus. sp: specimen, ar: steel arm guide, b: bearing block, h: hook

R.H. for a month before the test.

Test Specimen Configuration and Test Apparatus

Test specimen configuration is shown in Fig. 3, in which the variables are as follows.

The glue line lengths denoted by l are 5, 8, 11, 14, 17, and 20 cm.

The glue line thicknesses denoted by T are 0.01, 0.03, 0.075, and 0.15 cm.

Since the specimen has constant total length of 25 cm (denoted by L in Fig. 3), length of the unbonded region simulated as *crack* (denoted by a) is ranged from 5 cm to 20 cm.

Five same specimens were prepared on each glue line thickness and *crack* length, and thus the specimens totalled 120. Another dimentions of specimen were constant through the all specimens.

The schematic diagram of test apparatus is shown in Fig. 4. When center adherends are pulled down with tensile force 2P, outer two adherends are pushed up with two reaction forces 2×P on the steel bearing blocks b. Thus the symmetrical shear loading condition in which the rotating moments were vanished each other was realized. Moreover, the outer two adherends were prevented from buckling by means of loose holding of steel arm guides *ar*.

Determination of The Loading Point Displacement

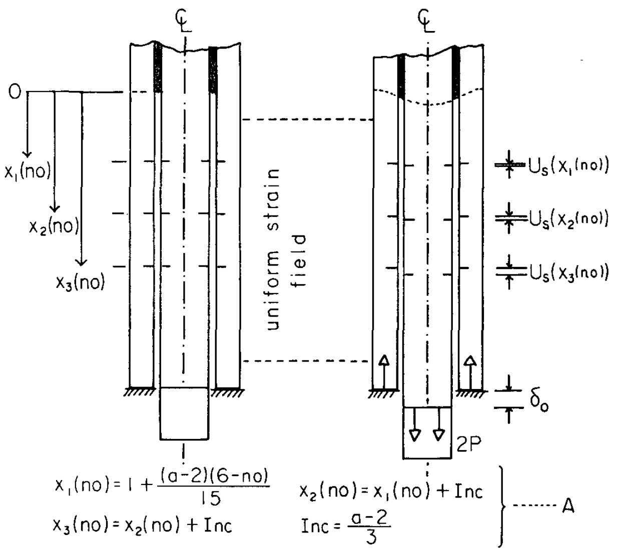

Fig. 5. Schematic diagrams of measurement of relative displacement.
a : *crack* length in cm, no : number of specimen arbitrary put from 1 to 5 on the five same specimens, U_s : relative displacement, δ_0 : loading point displacement

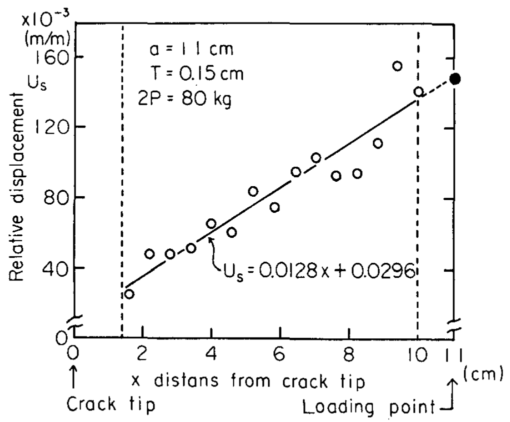

Fig. 6. An exsample of extraporation of the loading point displacement.

In this study the well-known compliance method originally developed by IRWIN and his associates[2] was used to evaluate the Fracture Toughness G_c. When the compliance method is used experimentally, the loading point displacement must be known to obtain the compliance as function of the specimen geometries.

In case of the specimen used in this study, plastic deformation at the vicinity of loading points was not small enough, it was, therefore, necessary to eliminate the plastic deformation from the loading point displacement to calculate the elastic strain energy stored in the specimen under the external load. For the elimination, the linear extrapolation of the relative displacement observed at uniform strain region was applied. In the specimen, the uniform strain was observed over the unbonded part except the vicinities of *crack* tip and loading points. Thus the relative movement of *crack* contours between the center and outer two adherends belonged to the uniform strain field was directly measured with the optical rule. The measurements were made on the razor cut marks at three appointed locations along each *crack* contour as shown in Fig. 5.

The cross head of the testing machine (TOM-200J, Shinkoh Communication Ind. Ltd.) was stopped at intervals of 20 or 25 kg to measure the relative displacement. The cross head speed was 1 mm/minute throughout the experiments.

The razor cut marks, at which the relative displacements (U_s) were measured, were made at different locations for the same five specimens in accordance with equation-A in Fig. 5.

For a certain *crack* length (a), glue line thickness (l), and load (2P) thirty relative displacements (U_s) measured on five same specimens were obtained, and then the paired values of U_s measured at the same horizontal locations but on different *crack* contours were averaged. Then, these fifteen averages were plotted against the locations from the *crack* tip as shown in Fig. 6. Finally, the least squares technique was employed to get a regression line from which the idealized elastic displacement (δ_0) at loading point could be obtained. All these operations were done on a FACOM 230-75 computer.

Compliance Method

The relation between load (2P) and loading point displacement (δ_0) obtained by the method described above are shown in Fig. 7(a)$\sim$(d). The compliance (δ_0/P) was evaluated from the inclination of fitted lines drawn on the plots, provided that linear relationship was held at least in the intermediate range of load (i.e., 2P=50$\sim$100 kg). The values of compliance obtained experimentally are shown in Table 1. The compliance for thick glue line (T=0.15 cm) was also calculated by numerical analysis of the Finite Element Method (F.E.M.) and is also shown in the table for comparison with the experimental value.

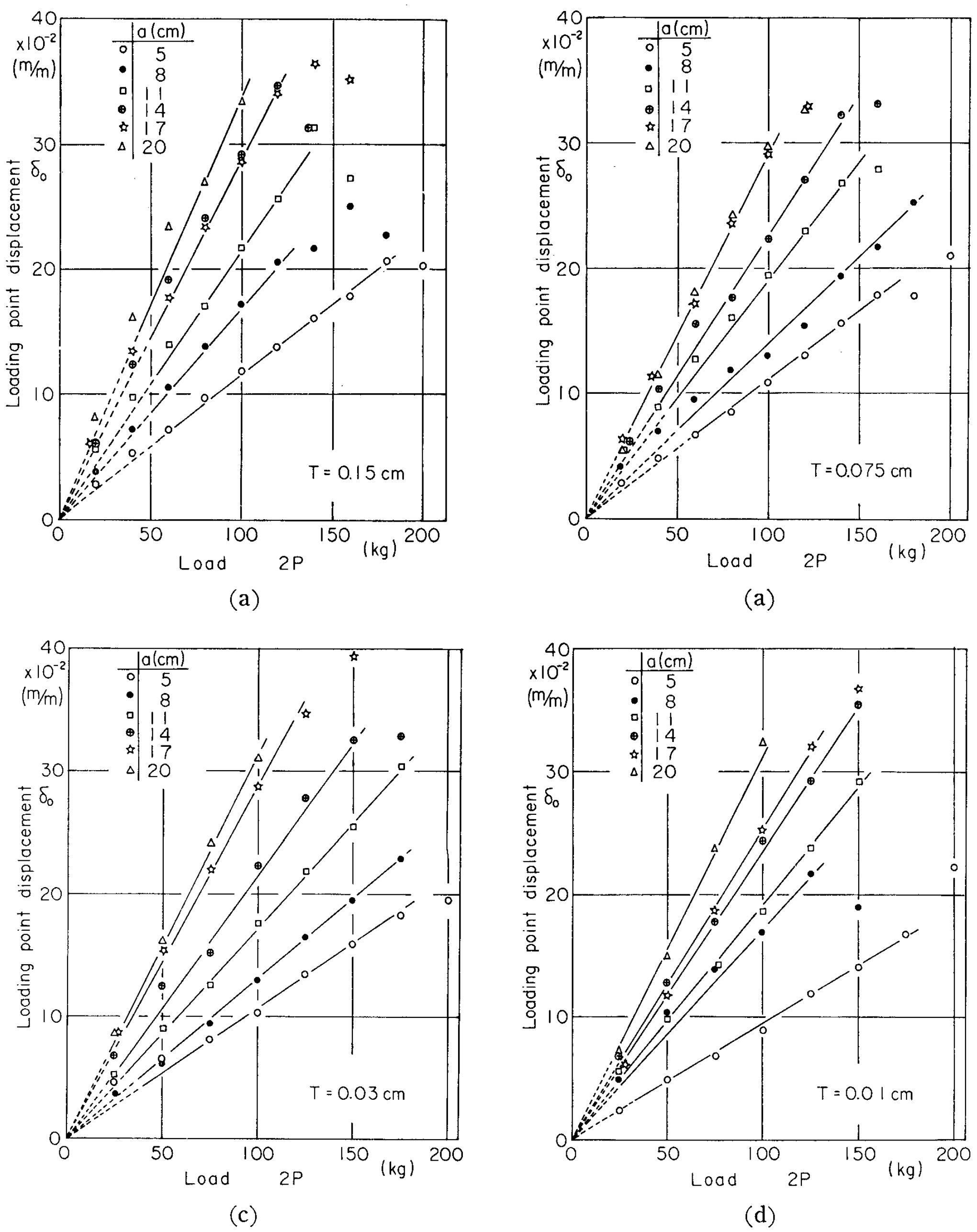

Fig. 7 (a)~(d). Relation between load ($2P$) and loading point displacement (δ_0).

From preliminary consideration, we recognized that in the specimen used it did not lead to reasonable results to use the compliance which was related only to the *crack* length. Therefore the glue line length (l) was combined with *crack* length (a) so as to make the effects of deformation of bonded region involve in the whole compliance ostensibly. A dimensionless ratio of a/l was selected as the most simplest combination.

Fig. 8 shows the relation between compliance (δ_0/P) and dimensionless ratio (a/l). After the iterative fitting operations for all of glue line thicknesses, the most simplest

Table 1. Values of compliance (δ_0/P) for different *crack* lengths (a) and glue line thicknesses (T).

T (cm) \ a (cm)	5	8	11	14	17	20	
0.15	23.0	33.4	42.8	57.2	57.2	66.8	
0.15	25.0*	34.0*	42.4*	51.1*	59.8*	68.8*	
0.075	22.2	27.8	38.0	45.2	58.4	58.4	$\times 10^{-5}$ (cm/kg)
0.03	21.6	26.0	34.4	43.2	58.0	63.4	
0.01	19.2	34.0	38.0	46.8	50.4	62.4	

* Values obtained by F.E.M.

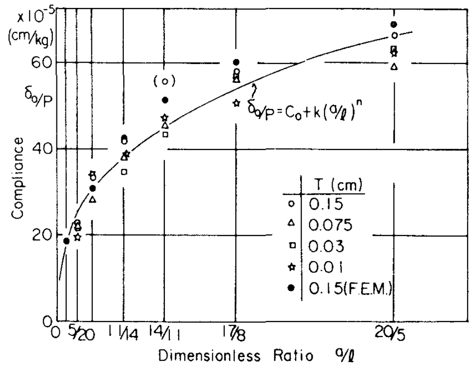

Fig. 8. Relation between compliance (δ_0/P) and dimensionless ratio (a/l).

regression equation was determined as follows.

$$\delta_0/P = C(a, l) = C_0 + k(a/l)^n \qquad \cdots\cdots\cdots\cdots(1)$$

Since the compliance C is a function of a and l, the compliance derivation is:

$$dC/da = \partial C/\partial a + (\partial C/\partial l)\cdot(dl/da) = \partial C/\partial a - \partial C/\partial l \qquad \cdots\cdots\cdots\cdots(2)$$

where, $l = L - a$

Substituting equation 1 in equation 2

$$\frac{dC}{da} = \frac{nkL}{al}(a/l)^n \qquad \cdots\cdots\cdots\cdots(3)$$

Then the Fracture Toughness G_c can be written:

$$G_c = \frac{P_c^2}{2H}\left(\frac{dC}{da}\right) = \frac{nkP_c^2}{2H}\cdot\frac{al}{L}\cdot(a/l)^n \qquad \cdots\cdots\cdots\cdots(4)$$

where H is thickness of specimen, P_c is half value of critical tensile force acting on center adherends, and n and k are coefficients determined by the iterative fitting, and in this study n and k were 0.4, 35.148×10^{-5} respectively for all glue line thicknesses.

Results and Discussion

Invariability of G_c

The Fracture Toughness G_c calculated from equation 4 for different *crack* lengths are shown in Fig. 9. It is recognized that the Fracture Toughness estimated are invariable for all different *crack* lengths tested. Thus the application of Fracture Mechanics to the adhesive system under external shear force is tolerable. The effects of glue line thickness on the G_c are scarcely recognized in the extend of this test. From these results, we adopted the value of 0.25 (cm•kg/cm^2) as the Fracture Toughness of wood (Lawson cypress)-Epoxy resin (flexibilizer free) adhesive system under external shear force. These results may not be compared with any other results directly, because no investigations have been done with respect to the system having the same loading conditions and materials.

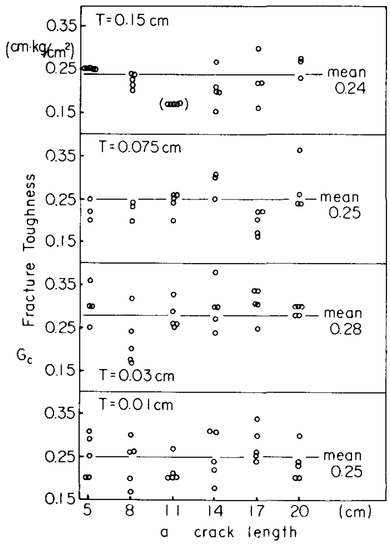

Fig. 9. Fracture Toughness G_c for different *crack* lengths and glue line thickness.

The only one which is narrowly possible to compare with respect to material condition under similar category of loading condition is the results of RIPLING et al.[4], in which test was done on Aluminum-Epoxy system. From simple comparison between the present results and theirs, it is recognized that G_{IIc} for the Aluminum-Fpoxy system with natural sharp crack inbeded in adhesive layer is at least one order of magnitude larger than G_c for wood-Epoxy system with narrow cavity simulated as *crack*. Results obtained by RIPLING et al. are shown in Table 2 with comparison of the present results.

On the other hand, the comparison with respect to the loading condition under the same adhesive system is possible. SASAKI[10] obtained G_{Ic} for wood-epoxy system under cleavage force with double cantilever beam specimen. The average values of G_{Ic} was

Table 2. Values of Fracture Toughness for various adhesive bonding systems.

System	Fracture Toughness cm•kg/cm²		Glue line thickness cm	Investigators
Lawson cypress (12 % M.C.)-(Cast Type) 11D/20 Epoxy*-same wood	G_c	0.24 0.25 0.28 0.25	0.15 0.075 0.03 0.01	Present test
2024-T4 Aluminum-(Budd Photostress Type A) Epoxy resin-same Aluminum	G_{IIc}	4.5 4.9 2.5 6.8	0.04 0.045 0.07 0.12	RIPLING et al.[4]
Mountain ash (13 % M.C.)-(Cast Type) 11D/20 Epoxy-same wood	G_{Ic}	0.18 0.24 0.19 0.19 0.19	0.0125 0.075 0.15 0.30 0.45	SASAKI[10]
Plexyglass-(ED6) 8~10P/50~60 Epoxy-Stell	G_{Ic}	0.04 0.017 0.06	neglected	MALYSHEV, SALGANIK[5]
2024-T351 Aluminum-(Dow 332) 10T/82 Epoxy-same Aluminum	G_{Ic}	0.06	0.0254	TRANTINA[6]
Aluminum-(DER 332) 12.5T/132 Epoxy-same Aluminum	G_{Ic}	0.12 0.19	0.0127 0.0635	MOSTOVOY et al.[9]

* Adhesives are identified as follows;

Bracket: general or commercial name of base resin.
First number: phr of hardner.
Letter: hardners' capital i.e. T=TEPA, D=DETA, P=PEPA.
Second number: post-cure temperature in °C.

0.2 ranging from 0.18 to 0.24 in cm•kg/cm² as shown in Table 2. This previous results indicate that the Fracture Toughness of wood-epoxy system is scarcely different in two cases of external shear and cleavage force conditions. About this, discussion will be made later with relation to the stress distribution at the vicinity of *crack* tip.

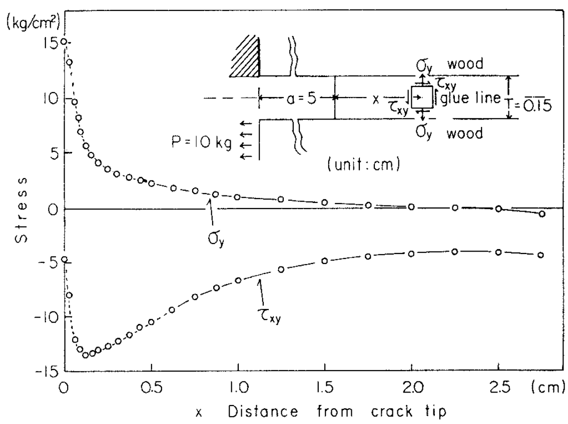

Fig. 10. Distribution of σ_y and τ_{xy} along the center of bond.

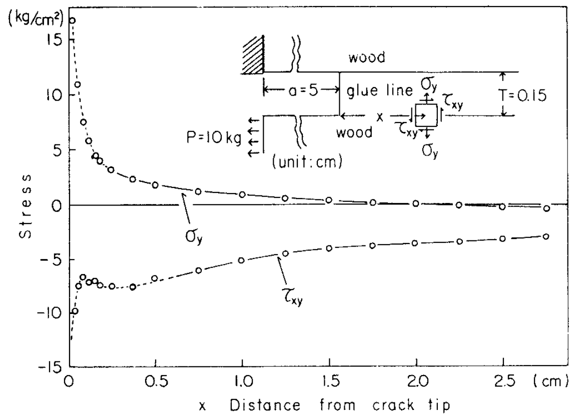

Fig. 11. Distribution of σ_y and τ_{xy} along the interface between adhesive and center adherend.

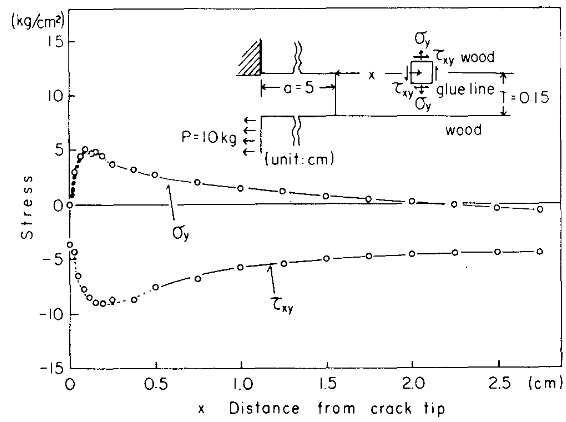

Fig. 12. Distribution of σ_y and τ_{xy} along the interface between adhesive layer and outer adherend.

As another comparison, some representative values of Fracture Toughness for various types of adhesive systems are also shown in the table.

Effects of Stress Component on Fracture

Numerical stress analysis by the usual Finite Element Method (F.E.M.) was done to determine the stress distribution near the *crack* tip (see Appendix-1). Fig. 10~12 show typical pattern of stress distribution at a certain *crack* length and glue line thickness. From these, it is shown that the most significant stress components which will participate in fracture are σ_y and τ_{xy} distributing along the interface of adhesive layer and center adherend, and the pattern of stress distribution along the interface of two

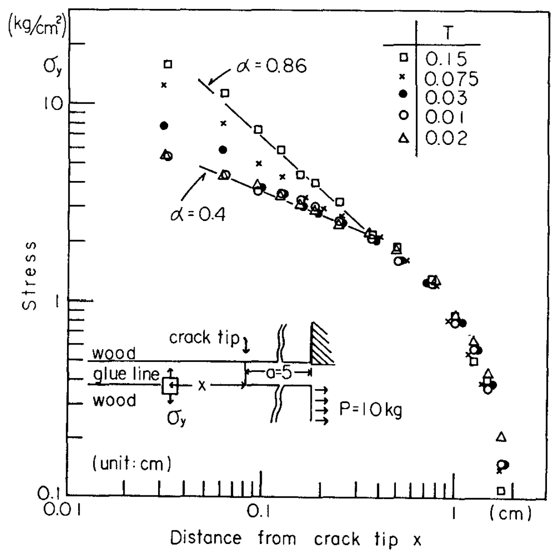

Fig. 13. Singularity and intensity of σ_y distributing along the interface between adhesive layer and center adherend.

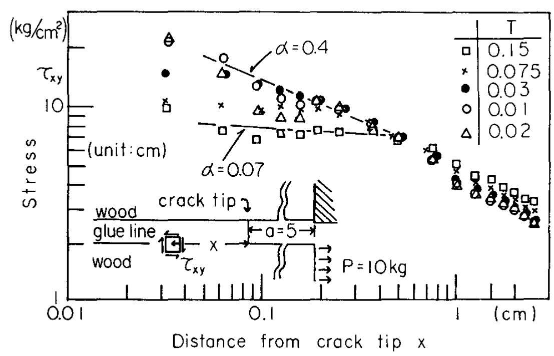

Fig. 14. Singularity and intensity of σ_{xy} distributing along the interface between adhesive layer and center adherend.

different materials at the vicinity of a right angle corner is not similar to that of homogeneous materials[12,13].

Fig. 13 and 14 show the effects of glue line thickness on the stress concentration of σ_y and τ_{xy}. In these graphs, "α" indicates the singularity of stress concentration from which the magnitude of participation of stress components in fracture might be deduced, if the stress distribution at vicinity of the *crack* tip could be assumed as equation 5 similar to that of homogenious materials[12].

$$\text{Stress} = K \cdot (1/x^{\alpha}) \qquad \cdots\cdots\cdots\cdots(5)$$

where, x is distance from the crack tip, K is stress intensity factor.

From this simplifying, in case of thick adhesive layer cleavage stress σ_y along the interface of adhesive layer and center adherend is the most dominant component, while in case of thin adhesive layer both cleavage σ_y and shearing stress τ_{xy} cope with each other. In reality, it was observed that fracture of 97~98% specimens tested initiated at the interface of adhesive layer and center adherend. It seems that the scatter of G_c for relatively thick adhesive layer was caused by the occasional contribution of cleavage mode of fracture. It was, however, not evident from the experiment that which mode of fracture, cleavage or shear would be more dominant throughout the test series on glue line thickness. At any rate, the combined mode of fracture would occur throughout all specimens.

Conclusions

1) The Fracture Toughness G_c of wood-epoxy system under the external shear force could be evaluated by employing the experimental compliance method. Although the values of G_c obtained were slightly variant through the series of glue line thickness tested, there were no essential distinctions.

In consequence, the value of 0.25 in cm·kg/cm^2 was taken as reasonable value of G_c with respect to the wood-epoxy resin adhesive system used in this study.

2) It seems that almost fractures of specimens tested were caused by combined contribution of cleavage and shearing stress components distributing along the interface of adhesive layer and center adherend.

Appendix-1

Finite Element Method

The finite element representation used in this study is shown in Fig. A1. In this figure, three kinds of element having different mechanical properties are used, i.e., wood element, epoxy resin element and *crack* element and their mechanical properties are shown in Table A1. In Fig. A1, when a certain *crack* length is desired, the finite element group near the *crack* tip was automatically exchanged by that of part ② including part ③ so as to fit the center of part ③ to the *crack* tip changing the mechanical properties of elements.

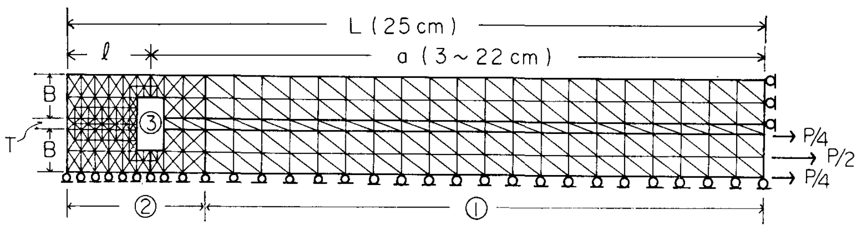

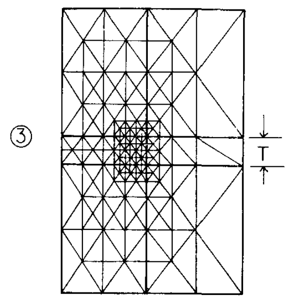

Fig. A1. Finite element representien of the test specimen used in this study (symbols to be refered to Fig. 3).
① : coarse mesh region
② : semi fine mesh region
③ : fine mesh region
number of element: 674
number of nodal points: 372

Table A1. Mechanical properties of materials used in F.E.M.

	Modulus of elastisity kg/cm²		Modulus of rigidity kg/cm²	Poisson's ratio	
	E_L	E_T	G_{LT}	μ_{LT}	μ_{TL}
WOOD	15×10^4	85×10^2	84×10^2	0.37	0.021
EPOXY	25×10^3		86.5×10^2	0.445	
GRACK	0		0	0	

The displacement method which has a shape function of first order was used and stress at a certain nodal point was calculated by averaging stresses in all elements which relate to the nodal point.

The linear simultaneous equations were resolved with the Gauss-Seidel B.S.O.R. technique. All computations were done on a FACOM 230-75 computer at the computer center of Kyoto University.

References

1) A. A. GRIFFITH, Philosophical Transactions of the Royal Society of London, **221**, 163 (1920).
2) G. R. IRWIN, Handbuch der Physik 6, p. 555, Splinger Verlag (1958).
3) M. L. WILLIAMS, J. Appl. Polymer Sci., **13**, 29 (1969).
4) E. J. RIPLING, S. MOSTOVOY, R. L. PATRICK, Materials Research & Standars, **4**, 129 (1964).

5) B. M. MALYSHEV, R. L. SALGANIK, International J. Fracture Mechanics, **1**, 114 (1965).
6) G. G. TRANTINA, J. Composite Materials, **6**, 192 (1972).
7) G. G. TRANTINA, ibid, **6**, 371 (1972).
8) S. MOSTOVOY, E. J. RIPLING, J. Appl. polymer Sci., **10**, 1351 (1966).
9) S. MOSTOVOY, E. J. RIPLING, J. Adhesion, **3**, 125 (1971).
10) H. SASAKI, Settchaku (Adhesion and Adhesives), **18**, 172 (1974).
11) P. F. WALSH, R. H. LEICESTER, A. RYAN, Forest Product J., **23**, 30 (1973).
12) R. H. LEICESTER, The Proceedings of the Second Austlarian Conference on Mechanics and Materials, p. 4.1～4.20 (1969).
13) M. L. WILLIAMS, J. Appl. Mechanics, **19**, 526 (1952).